19

Solid State and Thermal Behavior of 17β-Estradiol in Ammonioethyl Methacrylate Ester Copolymer

Chutima Wiranidchapong
Faculty of Pharmacy, Srinakharinwirot University
Thailand

1. Introduction

17β-estradiol is the most potent form of naturally occurring estrogen secreted during the reproductive years (Andersson 2000; Paoletti 2001). It is an essential steroid hormone that regulates numerous endocrine functions through binding to two estrogen receptor (ER) isoforms, i.e., ERα and ERβ. The concentration of these receptor subtypes and the corresponding cofactors vary with tissue types, leading to tissue specific regulation of estrogen response and toxicity. However, the content of ER in tissues has been assumed to be time-invariant (Plowchalk 2002). This indicates that multiple or prolonged exposure to E_2 of ER in various tissues should not alter physiological and toxic responses.

Estradiol (E_2) is carried in the plasma in two forms, bound to plasma binding proteins (95-98 %) and unbound form or free estradiol (2-5 %) (Dunn 1983; Pardridge 1986; Plowchalk 2002). Both unbound and bound forms of E_2 manifest pharmacological actions. Bound form acts as a reservoir for E_2 in blood circulation (Plowchalk 2002). After menopause the primary circulating estrogen is estrone, which is less biologically active than E_2 (Kuhl 2005; Margolis 2010). Thus, E_2 is usually administered to control early menopausal symptoms such as hot flashes and night sweats. For long-term administration E_2 can prevent cardiovascular diseases and osteoporosis (Andersson 2000; Paoletti 2001). After administered E_2 reaches to blood circulation, it rapidly undergoes chemical conversions to estrone, driven in part by the body's need to maintain homeostasis. Other estrogens in conjugated forms either equine- or synthetic-derived also exist as a balance between the ingested form and estrone at steady state in the body. Margolis (Margolis 2010) indicated that the conversion of E_2 to estrone was reversible reaction. Therefore, estrone plays as a hormonally inert reservoir, capably converting to E_2. These conversions make the administered estrogen indistinguishable from naturally occurring E_2 in the body.

However, hormone therapy is not without risks. The FDA and several professional organizations currently recommend prescribing the lowest effective dose for the shortest duration of time in accordance with treatment goals for an individual woman (Mueck 2003; Utian 2008; Margolis 2010). Nowaday there are a wide variety of estrogen products, including oral tablets, transdermal patches, and topical sprays, gels, and lotions, as well as vaginal creams, tablets, and rings. Selection of an appropriate product is often based on patient's preference. Oral estrogen dosage form is preferred due to its convenient route of

administration. To improve outcome of estrogen therapy, formulation properties and product pharmacokinetics should be considered for choosing an appropriate product.

2. Biopharmaceutics and pharmacokinetics of estrogen products

Oral administration of estrogen in tablet dosage form is the most favorable form for estrogen replacement therapy. The oral bioavailability of estrogen is dependent on its solubility in gastrointestinal (GI) fluid and permeability across membrane of endothelial cell lining in the gut wall. Unconjugated estrogens are hydrophobic molecules with low solubility in GI fluid. To improve the bioavailability their dissolution has to be increased. The methods normally used to enhance estrogen dissolution are chemical modification and reduction of the particle size.

Modification of chemical structure by conjugating with hydrophilic groups via esterification such as estradiol acetate and sulfonation such as sulfonated estrogens can improve drug dissolution. Conjugated estrogens exhibit better solubility than unconjugated form. However, most of conjugated estrogens have low affinity for ER. Thus, oral administration of conjugated form such as sulfonated estrogens may reduce undesired stimulation of ER within the GI tract. Since sulfonated estrogens are carried to target tissues, they are enzymatically hydrolyzed and then converted to bioactive estrogens (Margolis 2010). Similarly, estradiol acetate is also hydrolyzed in plasma and tissue and then transforms to active estrogen (Iwamori 2005; Margolis 2010).

Using micronized form of estrogen as an active ingredient in tablet formulation can improve estrogen dissolution by increasing surface area exposure to the dissolution medium. This phenomenon can be described by the Noyes-Whitney Equation (Shargel 1999);

$$\frac{dC}{dt} = \frac{DA}{h}(C_s - C) \quad (1)$$

where $\frac{dC}{dt} =$ rate of drug dissolution at time t, D = diffusion rate constant, A = surface area of the drug particles, C_s = concentration of drug in the stagnant layer (equal to solubility of the drug), C = concentration of drug in bulk solution, h = thickness of the stagnant layer.

From Noyes-Whitney equation, rate of drug dissolution at time t $\left(\frac{dc}{dt}\right)$ is directly increased as the surface area of the drug particles (A) is increased. Using micronized estrogen in tablet formulation results in the increase of surface area of the drug particles and consequently increases estrogen dissolution. Furthermore, design of tablet disintegration by using specific disintegrants in the formulation affects the duration to allow estrogen to dissolve in the GI fluid and then absorb into the blood stream. Product design potentially affects the bioavailability of estrogen.

During hormone therapy estrogens are orally administered once a day according to prolonged terminal elimination half-life (Plowchalk 2002). Oral dosage form of estrogens is often formulated in immediate-release tablet. This kind of product rapidly releases estrogen after administered. Due to rapid absorption of estrogens into the blood circulation (Margolis 2010), plasma estrogen concentration versus time profile reveals peaks and troughs pattern. Therefore, oral administration of immediate-release estrogen tablets has the potential to produce high spikes in blood levels, which possibly lead to estrogen-excess symptoms such as breast tenderness, headaches, nausea, vomiting, mood swings, bleeding, or spotting.

Boyd et al. (Boyd 2003; Margolis 2010) reported the decrease in maximum concentration ranging from 3% to 36% in a fed state as compared to a fasting state in subjects, taking

estrogen tablet with a high-fat meal. This report met an agreement with the reason of some patients undergone breakthrough hot flashes when taking their estrogen products with food (Margolis 2010). In addition, the variation of estrogen concentration in blood level probably comes from intestinal and hepatic first-pass metabolism of orally administered estrogen (Meli 1968; Longcope 1985; Plowchalk 2002). This characteristic results in low oral bioavailability of estrogen, which is only 2-5 % (Bawaarshi-Hassar 1989; Kuhnz 1993; Plowchalk 2002). Thus, trend of estrogen product development has been tempted to abandon oral administration and shifted to non-oral administrations.

Non-oral estrogen administration avoids hepatic first-pass effect, allowing smaller dose to be used and preventing undesirable changes from liver stimulation (Pentikis 1998; Munoz 1999; Rohr 1999; Andersson 2000; Paoletti 2001; Anderson 2002). However, desirable estrogen product is not only containing the lowest effective dose but also maintaining estrogen in blood level within a therapeutic range over a conveniently long dosing interval. These characteristics ensure adequate concentration of estrogen in blood for preventing both daytime hot flashes and night sweats, while not reaching overly high or peaky blood levels that may cause adverse events, such as breast tenderness, headache, nausea, vomiting, mood swings, bleeding, or spotting.

In the past, the only way to eliminate the peak and trough plasma levels of drug therapy was to deliver continuous intravenous (IV) infusion to a patient at a constant rate based on pharmacokinetics of the drug. However, this kind of drug administration requires health care professionals to monitor drug concentration in the plasma, thus usually cannot be performed at home. To alleviate this problem, various types of controlled-release drug delivery system have been developed to release the drug at a constant rate, replacing the administration via continuous IV infusion. In 1937, Parks and Dansby had formulated compressed pure crystalline estrogen pellets and administered them by subcutaneous injection to livestock. The results showed a continuous release of hormone over 3 months in several animals. Their work was presented at the Royal Society of Medicine in London. This led to a widespread idea of hormonal implantation in animals, which became the standard practice in the 1950s (Dash 1998). This discovery sparked an interest area of implantable drug delivery systems, leading to extended studies and continuous discoveries until the present time.

Implantable drug delivery systems have basically been classified into two major classes, i.e., drug implants and implantable pumps containing the drug. The first class utilizes various types of polymer matrices and polymeric membranes to control the kinetics of drug release from the delivery systems (Danckwerts 1991; Dash 1998). The second class consists of mechanical pump-type implants, which utilize an infusion pump-type action to control release of the drug. For estrogen therapy, the goal of the delivery system is to release estrogens at a constant rate throughout an intended period of time. Controlled release of estrogen products either transdermal patches or vaginal rings utilize polymer matrices and/or polymeric membranes as rate-controlling element similar to drug implants. To clearly understand how polymer matrices and polymer membranes can facilitate the release of estrogen, the fundamentals of rate-controlling drug delivery should be addressed.

3. Basic concepts of rate-controlled estrogen delivery

The majority of recent literatures have been focused on sustained-release and controlled-release drug delivery systems. Sustained-release drug product is referred to a dosage form formulated to retard the release of a therapeutic agent. Thus, the drug in the systemic

circulation is delayed the onset, prolonged its plasma concentration and provided longer duration of action (Chien 1992). On the other hand, controlled-release drug product is pointed to the delivery system giving a release profile not only predictable kinetically but also reproducible from one unit to another (Chien 1982; Chien 1989; Chien 1992).
Basic principles in the rate-controlled drug released from both polymer matrix and polymeric membrane is governed by Fick's laws of diffusion (Grant 1968; Chien 1992), which define the flux of diffusion (J_D) across a plane surface of unit area as shown;

$$J_D = -D\frac{dc}{dx} \tag{2}$$

where D is the diffusivity of drug molecule in a medium of solid, solution, or gas, $\left(\frac{dc}{dx}\right)$ is the concentration gradient of the drug molecule across a diffusional path with thickness dx, and a negative sign is used to define the direction of diffusion from a region with high concentration to a region with low concentration. The drug concentration gradient acts as the energy element for the diffusion of drug molecules.
In order to identify the mechanism of drug release, governed by Fick's laws of diffusion, the following assumptions need to be established (Chien 1992);

1. Dissolution of drug crystals into their surrounding medium is the first step of the drug release process.
2. A pseudo-steady state exists in the process of controlled drug release.
3. The diffusion coefficient of a drug molecule in a given medium is invariable with time and distance.
4. The interfacial partitioning of a drug molecule from polymer toward solution is related to its solubility in polymer (C_p) and in solution (C_s) as defined by

$$K = \frac{C_s}{C_p} \tag{3}$$

where K is defined as the partition coefficient.
Kinetically released of drug molecules from these types of rate-controlled drug delivery should be illustrated at each mechanism of drug release.

3.1 Polymer membrane permeation-controlled drug release

Polymer membrane permeation-controlled drug release has been appeared in a pharmaceutical dosage form in which a drug is totally or partially encapsulated within a drug reservoir compartment. The drug reservoir may exist in solid, suspension, or solution forms. The encapsulation of drug formulation inside the reservoir compartment is performed by spray coating, injection molding, hot-melt extrusion, microencapsulation, or other techniques.
The examples of this kind of rate-controlled drug delivery system are Progestasert IUD, an intrauterine device and Norplant, subdermal implant. Progestasert IUD contains a suspension of progesterone crystals in silicone medical fluid, encapsulated in a nonporous membrane of ethylene vinyl acetate copolymer in a T-shaped device. This product can continuously release progesterone in the uterine cavity at rate of at least 65 μg/day for a year (Chien 1992). For Norplant, the active drug is levonorgestrel, encapsulated in nonporous silicone medical-grade tubing with both ends sealed with medical-grade adhesive silicone. The development of this product has been found in 2 generations. The first is composed of 6 units of levonorgestrel crystals encapsulated in silicone tubes and the second is composed of 2 units of silicone tubes

containing levonorgestrel dispersing in silicone elastomer matrix inside. Both are designed to continuously liberate the active drug at a daily dosage rate of 30 μg for up to 7 years (Croxatto 1981; Weiner 1981; Diaz 1982; Segal 1983; Chien 1992).

The release process begins on the outermost layer of drug particles dissociating themselves from the crystal state and then dissolving in the surrounding medium, partitioning and diffusing through the polymer structure, and finally partitioning into the elution medium surrounding the device. During the device is sink in the surrounding medium, the hydrodynamic diffusion layer occurs on the immediate surface of the device. Therefore, the diffusion path length in which drug molecules diffuse across under a concentration gradient is the addition of the thickness of polymeric membrane and the hydrodynamic diffusion layer.

The cumulative amount of drug (Q) released from a unit surface area of a polymer membrane permeation-controlled drug delivery system is expressed as shown (Chien 1992);

$$Q = \frac{C_p K D_d D_p}{K D_d h_p + D_p h_d} t - \frac{D_p D_d}{K D_d h_p + D_p h_d} \int_0^t C_{b(t)}\, dt \tag{4}$$

where C_p is the drug solubility in the polymer, K is the partition coefficient as defined by Equation (3), D_p and D_d are the drug diffusivities in the polymer membrane with thickness h_p and in the hydrodynamic diffusion layer with thickness h_d, respectively. $C_{b(t)}$ is the concentration of drug in the interface of diffusion layer/ bulk solution, t is time, and dt is a differential length of time.

In the case of sink condition throughout the course of controlled drug release, the saturated concentration of drug in the solution (C_s) is much higher than the concentration of the drug in the bulk solution ($C_{b(t)}$); $C_s >> C_{b(t)}$ or $C_{b(t)} \approx 0$. Thus, Equation (4) can be reduced to

$$Q = \frac{C_p K D_d D_p}{K D_d h_p + D_p h_d} t \tag{5}$$

The rate of drug released from this system can be defined by rearrangement of Equation (5) into

$$\frac{Q}{t} = \frac{C_p K D_d D_p}{K D_d h_p + D_p h_d} \tag{6}$$

Equation (6) indicates that the rate of drug release per unit time is equal to a constant value, i.e., the solubility of drug in the polymer, the partition coefficient, the diffusivity of drug molecule, and the thickness of the rate-controlling membrane. This implies that the polymer membrane permeation-controlled drug delivery gives a constant drug release profile. Equation (6) has considerably described the release of progesterone from Progestasert IUD (Chien 1992).

In case of a thick polymer membrane (h_p) and/or extremely low diffusivity of drug molecules in a polymer (D_p), which is dependent on the type of polymer material, the term of $KD_d h_p$ is much higher than the term of $D_p h_d$. Thus, Equation (6) can be simplified to

$$\frac{Q}{t} = \frac{C_p D_p}{h_p} \tag{7}$$

Under this condition the rate of drug release is a function of the solubility and diffusivity of drug in the polymer and is inversely proportional to the thickness of the polymer membrane. So the release of drug molecules is governed by the membrane-modulated permeation process.

In case of a very low interfacial partition coefficient (K) or a thick hydrodynamic diffusion layer (h_d), in which a condition is little movement of the surrounding medium, the KD_dh_p term is significantly smaller than the D_ph_d term. Equation (6) can be reduced to

$$\frac{Q}{t} = \frac{C_pKD_d}{h_d} \tag{8}$$

From Equation (2), since $C_pK = C_s$, Equation (8) can be rewritten as;

$$\frac{Q}{t} = \frac{C_sD_d}{h_d} \tag{9}$$

Under this condition the rate of drug release is a function of drug solubility in the surrounding medium and drug diffusivity in the hydrodynamic diffusion layer and is inversely proportional to the thickness of the hydrodynamic diffusion layer. Thus, the release of drug molecules is governed by the diffusion layer-limiting partition-controlled process.

From the principle of controlled release of drug from a dosage form in which the drug is encapsulated inside the polymer membrane, solubility of the drug strongly affects the rate of drug release. Under the condition in which the polymeric membrane plays the leading role in modulation of drug release, drug solubility in that polymer is a significant factor influencing the rate of drug release. On the other hand, under the condition of the hydrodynamic diffusion layer-limiting partition-controlled process, drug solubility in the surrounding medium affects the rate of drug release. Thus, an alteration in drug solubility either in polymer membrane or in the surrounding medium can also affect the rate of drug released from this kind of drug delivery system.

3.2 Polymer matrix diffusion-controlled drug release

Delivery system, controlling drug release by polymer matrix diffusion-controlled drug release, is prepared by homogeneously dispersing drug particles in a rate-controlling polymer matrix. The drug dispersion in the polymer matrix can be produced by dissolving the drug and the polymer in an appropriate solvent, followed by solvent evaporation at an elevated temperature and/or under a vacuum, or mixing finely ground drug particles with a rubbery polymer at an elevated temperature. The drug-polymer dispersion is then compressed, molded, or extruded to form a drug delivery device of various shapes and sizes designed for specific application.

An example of this type of drug delivery system is Compudose subdermal implant, fabricated by dispersing micronized estradiol (E_2) crystals in a viscous silicone elastomer and then coating the E_2-dispersing polymer around a rigid (drug-free) silicone rod by extrusion to form a rod-shaped implant. This product has been used for growth promotion in steers. It can release E_2 at controlled dose for 200 to 400 days (Hsieh 1987; Chien 1992).

The release of drug dispersing in a matrix environment is based on the hypothesis that the drug particles cannot move from their individual positions in the polymer matrix. The drug solids in the layer closer to the surface of the device are first diffused, so that this layer becomes a drug depletion zone. Then, the drug particles in the next layer begin to dissolve and diffuse, resulting in the growing thickness of drug depletion layer. This thickness becomes greater and greater as more drug solids are eluted out of the device, leading to inward advancement of the interface of drug dispersion zone/ drug depletion zone into the core of the device for another thickness(dh_p). Therefore, the rate of drug release from the polymer matrix diffusion-controlled drug delivery system is time-dependent and

progressively decreases in response to increase in the thickness of the diffusional path as time goes by. At steady state the rate of drug release $\left(\frac{dQ}{dt}\right)$ is defined as followed (Chien 1992);

$$\frac{dQ}{dt} = \left(\frac{AC_pD_p}{2t}\right)^{\frac{1}{2}} \tag{10}$$

where A is the initial drug loading dose in the polymer matrix, C_p is the drug solubility in the polymer, which is also the drug reservoir concentration in the system, and D_p is the diffusivity of the drug molecules in the polymer matrix.
Integration of Equation (10) gives the relationship of the cumulative amount of drug release (Q) directly varied with the square root of time as the following equation;

$$Q = \left(2AC_pD_p\right)^{\frac{1}{2}}(t)^{\frac{1}{2}} \tag{11}$$

From Equation (11), the cumulative amount of drug released from the polymer matrix diffusion-controlled drug delivery system is controlled by the loading dose, solubility and diffusivity of the drug in the polymer matrix. This confirms that the drug solubility in the polymer is also one of significant factors affecting the amount of drug released from this delivery system.
One major drawback of the polymer matrix diffusion-controlled drug delivery system is its inability to achieve a constant release due to the variable thickness of the drug depletion zone. The thickness of the drug depletion zone increases as the release of drug proceeds. Therefore, the rate of drug release decreases with the reciprocal of the square root of time. Rippe and Johnso (Rippie 1969), Cobby et al. (Cobby 1974), and Hsieh et al. (Hsieh 1983) revealed that the shape of a matrix could be a factor affecting drug release, so that several researches since last 2 decades have been done in development of new designs of matrix system in order to achieve the zero-order or near zero-order release kinetics.

3.2.1 Hemipheric polymer matrix diffusion-controlled drug release

Drug released from hemispheric polymer matrix device has been designed to achieve a constant release (Hsieh 1983). The device is composed of the drug dispersing in a hemispheric polymer matrix, coated with an impermeable material except for a small cavity cut into the center of the flat surface as shown in Figure 1. Only a cavity in the center where

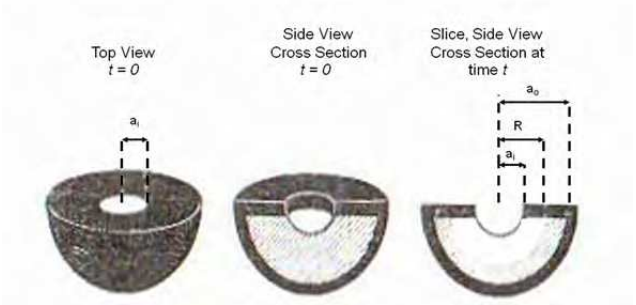

Fig. 1. Diagram of a hemispheric polymer matrix device: a_i was the inner radius; a_o was the outer radius; R was the distance to the interface between the drug depletion zone (white area) and the drug dispersing zone (diagonal lines); and black represented coated regions through which the drug release could not occur (From Hsieh, et. al., 1983).

the drug can be released the interface between drug depletion zone and drug dispersing zone moves into the interior as a front. The inwardly-releasing hemisphere increases the available area, where the drug can be released, so as to compensate the increase in diffusion distance of drug transport.

The rate of drug release $\left(\frac{dQ}{dt}\right)$ from the hemispheric polymer matrix device can be expressed as (Hsieh 1983);

$$\frac{dQ}{dt} = 2\pi C_s D_p a_i \left(\frac{R}{R-a_i}\right) \tag{12}$$

where π is a constant value, C_s is drug solubility in the surrounding medium, D_p is the diffusivity of drug molecules in the polymer matrix, a_i is radius of the cavity, and R is radial distance to interface between drug depletion zone and drug dispersing zone within the matrix.

Since R-a_i becomes equal to R when $R \gg a_i$. Equation (12), then, can be simplified to;

$$\frac{dQ}{dt} = 2\pi C_s D_p a_i \tag{13}$$

Each of the terms in Equation (13) is a constant. Thus, the rate of drug released from the hemispheric polymeric matrix device with small a_i is essentially constant. The theoretical analysis has been agreed with the experimental data obtained from Hsieh et al. (Hsieh 1983). Their study addressed that hemispheric matrices acted as constant release systems for both sodium salicylate and bovine serum albumin, which were represented as small molecule and macromolecule, respectively.

3.2.2 A hollow cylindrical polymer matrix diffusion-controlled drug release

Drug released from a hollow cylindrical matrix device demonstrates a constant release profile because mechanism of drug released from this device is almost similar to that of the hemispheric polymer matrix device. This device has been fabricated by Vandelli and Cameroni since 1993 (Vandelli 1993a; Vandelli 1993b). It is a cylindrical polymer-drug matrix with a hole bored in the center of the flat surface through both sides of the matrix as displayed in Figure 2. All surfaces of the device are coated with an impermeable polymer except a central hole where the drug can be released, similar to the hemispheric polymer matrix device.

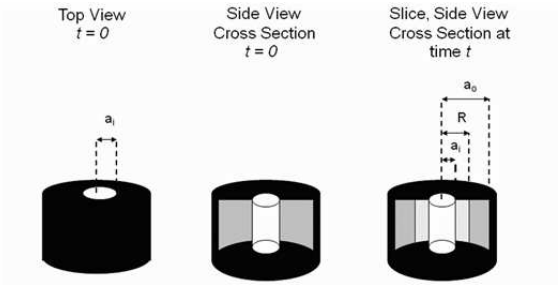

Fig. 2. Diagram of a hollow cylindrical matrix device: a_i was the inner radius; a_o was the outer radius; R is the distance to the interface between the drug depletion zone (light gray area) and the drug dispersing zone (dark gray area); and black representing coated regions through which the drug release could not take place (Reproduced from Wiranidchapong, 2006).

In addition, the swelling polymer used in the matrix can modulate the drug release following pseudo-zero order kinetics regardless of the loaded drug. This device regulates the drug release by swelling process and the effect of matrix geometry (Vandelli 1993b).

3.2.3 The three-layer polymer matrix diffusion-controlled drug release

The three-layer polymer matrix device has been designed to achieve zero-order kinetics of the drug release under the trade name of Geometrix® Technology since 1992 (Conte 1993; Conte 1996; Conte 2000; Abdul 2004). In fact, this device is a multi-layer tablet, which comprises of a matrix core containing an active drug and one or more barriers applied to the core directly during the tableting process. The barriers reduce the burst release of the drug in the core by limiting the available surface for the drug release and controlling the solvent penetration rate at the same time. During the subsequent portions of the barriers dissolve, the erosion of these swollen barriers is dominated and the surface available for the drug release slowly increases. In this way the decrease of delivery rate due to the increase of diffusion path-length, corresponding to the increase of drug depletion zone, is counterbalanced by the simultaneous increase of the available area for drug release. Thus, the drug release can be maintained at a relatively constant level during the swelling and erosion of the barriers.

Maggi et al. (Maggi 2000) declared that release profiles of the three-layer matrices with the same cores and different barriers were different. The barriers containing polymers of higher viscosity were stronger reduction in the rate of drug release than those containing polymers of lower viscosity. In the same way, the cores containing the polymers of higher viscosity released the drug at a lower rate than those containing the polymers of lower viscosity. However, the dissolution profiles of the three-layer systems with the same barriers but different polymers used in the cores were similar. Their work was focused on the modulation of highly water-soluble drug released such as diltiazem hydrochloride. Therefore, the core had less effect on the modulation of drug release while the barriers played the leading role in controlling drug release from the three-layer matrix system used a highly water-soluble drug as a model drug.

The three-layer polymer matrix containing 17β-estradiol (E_2) as a model drug was produced by Wiranidchapong (Wiranidchapong 2006). E_2 dispersing in poly(ethyl acrylate-methyl methacrylate-trimethylammonioethyl methacrylate chloride) 1:2:0.1 or Eudragit® RS (ERS) at weight percent of 10, 20, and 30 was used in the core component while ERS free drug was used as polymeric barriers on both sides of the core. In vitro release of E_2 from the three-layer matrices exhibited 80 % of cumulative amount of E_2 released within 7 days in all cases as shown in Figure 3(a). E_2 daily release rate from these matrices is shown in Figure 3(b). The increase in weight percent of E_2 in the core did not significantly increase E_2 daily release rate.

To compare E_2 release profiles obtained from the three-layer matrices containing different weight percents of E_2 used in the cores, the similarity factor (f_2) was used in the assessment. The f_2 test adopted by the Center for Drug Evaluation and Research (FDA) and by Human Medicines Evaluation Unit of the European Agency for the Evaluation of Medicine Products (EMEA) can be defined as the following equation (Costa 2001).

$$f_2 = 50 \times log\left[\left\{1 + \left(\frac{1}{n}\right)\sum_{j=1}^{n}\left|R_j - T_j\right|^2\right\}^{-0.5} \times 100\right] \quad (14)$$

where n is the sampling number, R_j and T_j are the percent dissolved of two comparative formulations at each time point j. FDA and EMEA have suggested that two dissolution profiles are declared similar if f_2 is between 50 and 100. The higher f_2 value, the more similar dissolution profiles are obtained (Costa 2001).

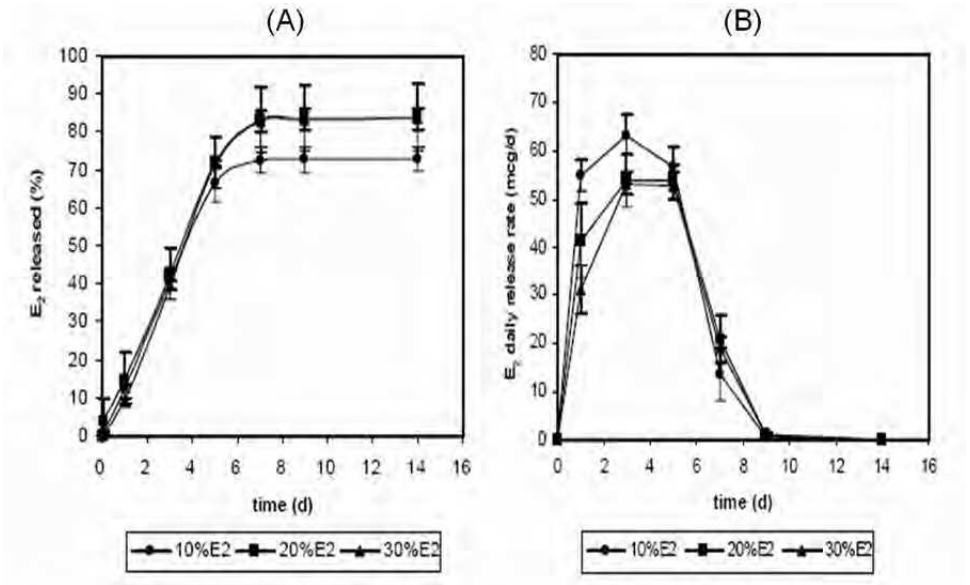

Fig. 3. In vitro release (A) and the daily rate (B) of E_2 released from the three-layer matrices containing 10, 20, and 30 % w/w E_2 in ERS used in the cores (Reproduced from Wiranidchapong, 2006).

f_2 values of E_2 release profiles of the core containing 10 % w/w E_2 compared with those containing 20 and 30 % w/w E_2 were 57.18 and 58.16, respectively. In addition, f_2 values obtained from the comparison of E_2 release profiles of the core containing 20 % w/w E_2 with those containing 30 % w/w E_2 was 77.77 (Wiranidchapong 2006). Thus, E_2 release profiles of the three-later polymer matrices containing 10, 20, and 30 % w/w E_2 in ERS used in the cores were similar.

In the case of the increase in weight percent of drug in the matrix, the porosity upon drug depletion is increased and the tortuosity is reduced, so that rate of drug release should increase. However, the rate of E_2 release did not increase as weight percent of E_2 in the cores increased. This suggested that the increase in porosity and the decrease in tortuosity in the core of the three-layer matrix could not elevate the E_2 release rate. The porosity and the tortuosity might not be the important factors in controlling E_2 release from this system.

Similar study was investigated with norethindrone (NET), the other poorly water-soluble drug, used in the core and ERS employed as barriers of the three-layer matrix (Wiranidchapong 2006). The cumulative release and the daily release rate of NET from the three-layer matrices containing 30, 40, and 50 % w/w NET in ERS used in the cores are shown in Figure 4. NET release profiles showed 80 % of NET released within 14 days in all cases. NET daily release rate exhibited relatively constant within 9 days.

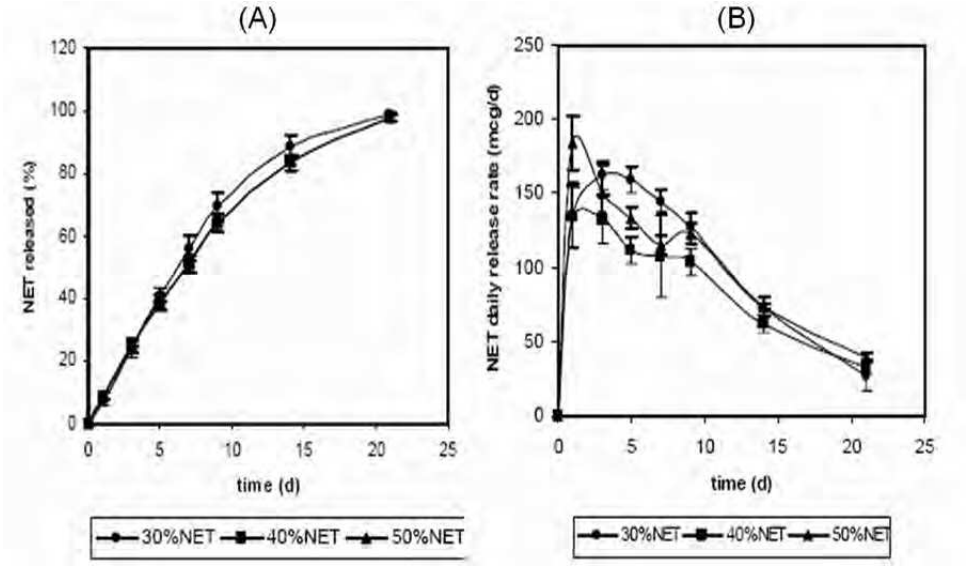

Fig. 4. In vitro release (A) and the daily rate (B) of NET released from the three-layer matrices containing 30, 40, and 50 % w/w NET in ERS used in the cores (Reproduced from Wiranidchapong, 2006).

From preliminary study conducted at 37°C, 120 rpm, the solubility of E_2 and NET in 3.5 % w/v benzalkonium chloride in phosphate buffer pH 7.4 used as release medium were 891.29 µg/ml and 460.16 µg/ml, respectively. The solubility of NET in the release medium is around two times lower than that of E_2 corresponding to two times longer extended release of NET than that of E_2.

The f_2 values obtained from the comparison of NET release profile of the three-layer matrix in which core containing 30 % w/w NET with those containing 40 and 50 % w/w NET were 73.23 and 72.55, respectively. Furthermore, f_2 values obtained from NET release profile of the core containing 40 % w/w NET compared with that of 50 % w/w NET was 96.69. This indicated the similarity among NET release profiles obtained from the three-layer polymer matrices containing 30, 40, and 50 % w/w NET in the polymeric cores.

This study represented that the intrinsic solubility of E_2 and NET affected the duration of drug released from the three-layer matrix. The increase in weight percent of E_2 and NET used in the core corresponding to the increase of the porosity and decrease of the tortuosity did not increase the daily release rate. The solubility of E_2 and NET in the release medium predominated in controlling the E_2 and NET release when compared with the porosity and the tortuosity upon drug depletion.

Further study was to investigate the effect of the barrier and the type of polymer used in the core and barrier on NET released from the three-layer matrix (Wiranidchapong 2006). Poly(ethyl acrylate-methyl methacrylate-trimethylammonioethyl methacrylate chloride) 1:2:0.1 and 1:2:0.2 or Eudragit® RS (ERS) and Eudragit® RL (ERL), respectively have been used as rate controlling polymers. ERL is more permeable than ERS because of higher content of quaternary ammonium groups in the structure. The NET released profile obtained from the three-layer matrix using ERL in the core was compared with that of ERS.

In addition, the NET released profiles obtained from the three-layer matrices having the same cores but different kinds of polymer used in the barriers and without the barriers were also investigated. The percentage of drug loading was set at 30.
The cumulative release of NET from the three-layer matrices using ERL in the cores with barrier layers of either ERL or ERS exhibited 80 % of NET released within 2 days whereas those of ERS in the cores with either ERS or ERL in the barriers and without the barriers exhibited 80 % of NET release within 14 days as illustrated in Figure 5. The difference of polymer used in the core significantly changed NET release profile but the difference of polymer used in the barriers, including without the barriers did not significantly change NET release profile. Therefore, the core exerted more influence on the modulation of a poorly water-soluble drug release than the barrier did.
NET release profiles of the devices containing ERS in the cores were compared with each other. The f_2 values of NET release profiles obtained from the device using ERS in the barriers compared with those of ERL and without the barriers were 75.36 and 77.76, respectively. In addition, f_2 value of NET release profile obtained from the device using ERL in the barriers compared with that of without barriers was 86.00. The NET release profiles obtained from the devices using ERS in the cores with the barriers using either ERS or ERL and without the barriers were similar. Thus, the three-layer design did not affect the NET release.

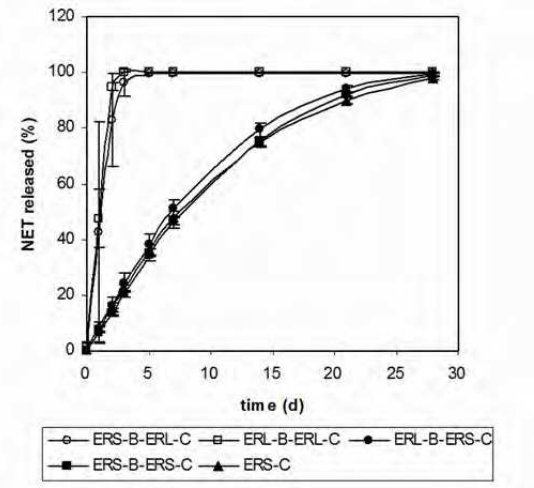

Fig. 5. In vitro release of NET from the three-layer matrices containing ERS or ERL used in the cores and ERS or ERL used in the barriers, including without the barriers (Reproduced from Wiranidchapong, 2006).

Approximately 60 % of either E_2 or NET released from the three-layer matrices investigated in this study were well fitted with the zero-order released model by linear regression analysis. The coefficient of determination (R^2) obtained from each fit was in the range of 0.9946 – 0.9999 (Wiranidchapong 2006). The zero-order model was apparently appropriate to describe either E_2 or NET released from the matrices using ERS as the rate-controlling polymer. As previously mentioned, the zero-order kinetic of drug released is accomplished in the polymer membrane permeation-controlled drug delivery system in both conditions

governed by the polymeric membrane-modulated permeation process and the diffusion layer-limiting partition-controlled process. In case of incompletely coated membrane such as the three-layer polymeric matrix, the hydrodynamic diffusion layer (h_d) predominates in controlling the drug release. As seen in Equation (9), the rate of drug release is a result of drug solubility in the surrounding medium.

Chandrasekaran and Paul (Chandrasekaran 1982) announced that the solubility of poorly water-soluble drug predominated and offered as the limiting resistance to drug release. This resulted in the saturated concentration of dissolved drug at the inside of matrix pores when drug loading exceeded the drug solubility under the given condition. Non-dissolved drug was not available for diffusion but it acted as a drug reservoir for keeping constant the absolute amount of drug release within a certain period of time. The zero-order release kinetic could be achieved under this condition (Siepmann 2001). Furthermore, Kim (Kim 2000) indicated that the geometry was not an important factor for a drug dissolution controlled release system and the increase in the porosity and the reduction in the tortuosity did not influence the kinetics of drug release. Therefore, the zero-order kinetic of either E_2 or NET released from the matrices was a result of the inherent solubility of E_2 and NET providing the drug dissolution controlled release system (Wiranidchapong 2006).

The E_2 released from the polymeric matrix is controlled by the dissolution of E_2 in the surrounding medium. Therefore, an alteration in the solid state of E_2 dispersing in the polymer matrix can modify the characteristic of E_2 release. Solid state of E_2 should be revealed in both cases of pure drug and the drug dispersing in the polymer under various conditions, which might be appeared in the manufacturing process.

4. Solid state properties of estradiol

The most common form of E_2 is the hemihydrates (Variankaval 2000; Wiranidchapong 2008). However, E_2 can exist in various kinds of pseudopolymorphs as hemisolvates, dependent on the type of solvent used in the crystallization. For an example, E_2-hemisolvate of methanol was produced by crystallization in saturated solution of E_2 in methanol (Variankaval 2000). In addition, either polymorphs or pseudopolymorphs exhibit the definite arrangement of molecules inside the crystal lattice. This directly affects on a crystal habit, which is an external shape of the crystal. Thus, crystal morphology is a specific characteristic for each polymorphic form. An alteration in polymorphic state possibly changes the crystal habit and/or even crystal morphology, leading to significant variation in raw-material characteristics such as particle orientation, flowability, packing, compaction, suspension stability and dissolution. This can lead to serious implications of physical stability in dosage forms (Niazi 2007).

E_2 can exist in the amorphous form and at least three crystalline forms, including E_2-hemihydrate (Variankaval 2000; Wiranidchapong 2006; Wiranidchapong 2008). Differential scanning calorimetry (DSC) curve reveals that the three crystal forms and amorphous form of E_2 are inter-convertible under various thermal conditions as displayed in Figure 6(A) (Wiranidchapong 2006; Wiranidchapong 2008). This indicates that the polymorphic transformation of E_2 possibly occurs during manufacturing process in which optimal thermal energy has been utilized. Thus, inconsistency of E_2 polymorphs have probably been found in pharmaceutical products obtained from inadequate quality control of manufacturing procedures. Different polymorphs exhibit dramatic change in physical and chemical properties. This leads to inconsistency in dissolution rate, rate of drug release from

controlled-release product, and bioavailability. To control the product quality, physicochemical properties of E_2 polymorphs should be verified.

4.1 Characterization by DSC and TGA

From DSC analysis, E_2-hemihydrate exhibited the melting point onset at 179.2 °C corresponding to the third endotherm observed in the first heating run (DSC; 0-182 °C at 10 K/min). The first endotherm (onset at 110 °C) and second endotherm (onset at 174 °C) in the first heating run corresponded to the partial release of hydrogen bonded water and the complete loss of water lattice, respectively. The water loss observed in the first scan was agreed with a weight loss of 3.2 % of E_2 measured by thermogravimetric analysis (TGA) as illustrated in Figure 6(B) (Wiranidchapong 2006; Wiranidchapong 2008). This result indicated that the stoichiometry of E_2 should be $C_{18}H_{24}O_2.\frac{1}{2}H_2O$.

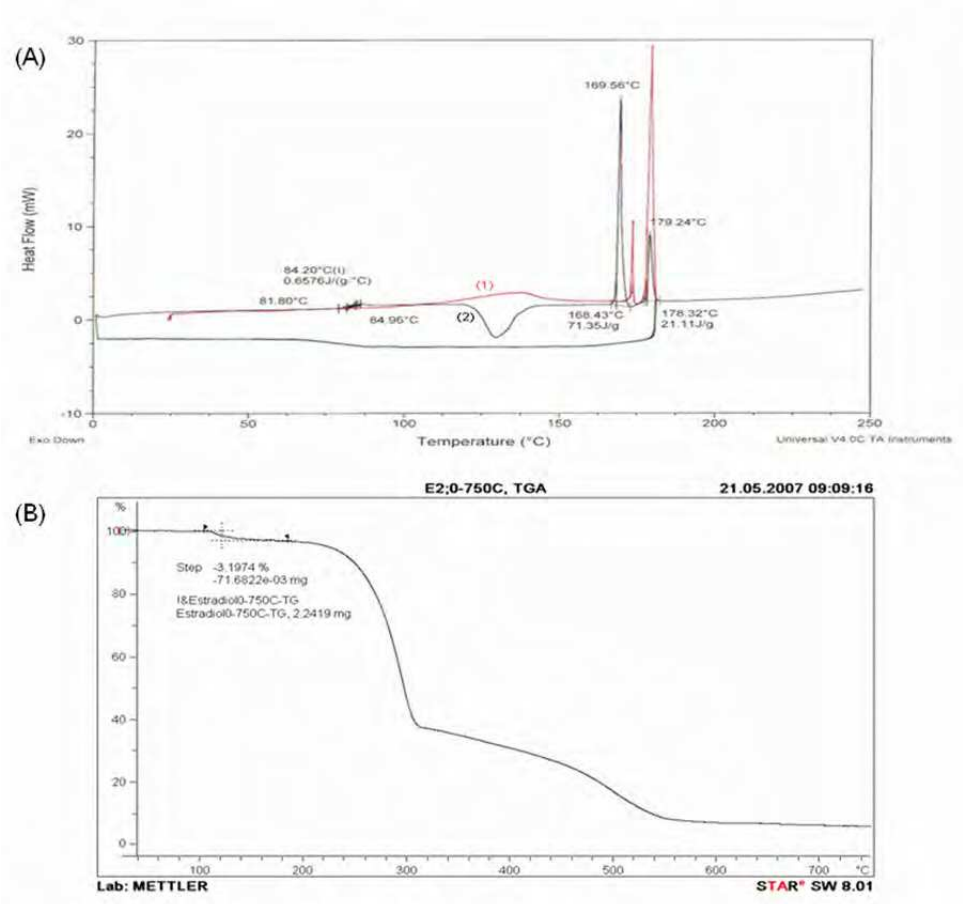

Fig. 6. (A) DSC curve of E_2 scanned with the program: (1) heating to 182 °C, 10 K/min, cooling to 0 °C, 20 K/min, and then (2) heating to 250 °C, 10 K/min; (B) TGA of E_2 (Reproduced from Wiranidchapong, 2008).

On cooling (DSC; 182-0 °C at 20 K/min) the glass transition temperature (T_g) was observed around 84.2 °C, correlating to that observed in the second heating (DSC; 0-250 °C at 10 K/min). This aspect revealed an appearance of amorphous E_2 after E_2-hemihydrate had been melted and then rapidly cooled. In the second heating the amorphous E_2 in glassy state was changed to that in rubbery state when the temperature reached the T_g, followed by recrystallization into ED form as stated by Variankaval et al. (Variankaval 2000) and anhydrous E_2 exhibiting their melting points at 169.6 °C and 179.2 °C, respectively (Variankaval 2000; Wiranidchapong 2006; Wiranidchapong 2008).

4.2 Characterization by X-ray powder diffraction

Each polymorph of E_2 exhibits the definite X-ray powder diffraction (XRPD) patterns as illustrated in Figure 7. E_2-hemihydrate demonstrates characteristic peaks at 13.14, 15.74, 18.26, 22.62, and 26.58° (Latsch 2003; Park 2005; Wiranidchapong 2006; Wiranidchapong 2008). Anhydrous E_2 prepared by heating E_2-hemihydrate from 0-175 °C and 0-180.5 °C at heating rate of 5 K/min exhibited the characteristic peaks at 13.60, 16.78, 21.00, and 24.72°, which were not observed in the diffraction pattern of E_2-hemihydrate.

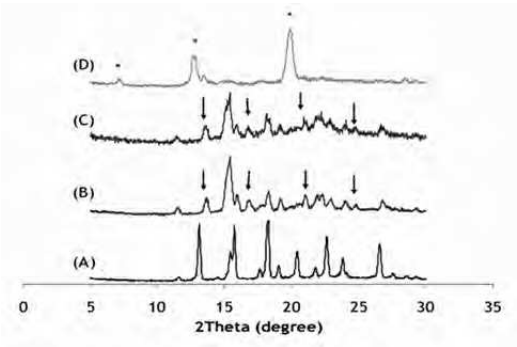

Fig. 7. XRPD of E_2-hemihydrate (A); anhydrous E_2 produced from either heating to 175 °C, 5 K/min (B); or heating to 180.5 °C, 5 K/min (C); and ED form of E_2 (D) (Reproduced from Wiranidchapong, 2008).

The relative peak intensity of anhydrous E_2 obtained from heating to 180.5 °C was less than that of anhydrous E_2 obtained from heating to 175 °C. In addition, the diffraction peaks of anhydrous E_2 obtained from heating to 180.5 °C did not significantly separate from baseline, indicating a mixture of crystalline form and amorphous form. This represents the inconsistency in the appearance of E_2 polymorph when the process slightly changes. ED form of E_2 prepared by heating E_2-hemihydrate to 180.5 °C at 5 K/min and cooling to 0 °C at 20 K/min and finally heating to 140 °C at 5 K/min manifested the definite diffraction pattern, which exhibited the characteristic peaks at 12.64 and 19.94°. This feature indicates that XRPD analysis can be used to investigate polymorphic forms of E_2, which are inter-convertible under various thermal conditions.

4.3 Characterization by FTIR

FTIR spectra of E_2-hemihydrate, anhydrous E_2, and the mixture of anhydrous E_2 with amorphous E_2 are displayed in Figure 8. E_2-hemihydrate exhibited very broad bands

centered at 3435.95 and 3232.06 cm^{-1} attributed to O-H stretching of hydroxyl group adjacent to C-17 and C-3 positions in E_2 chemical structure, respectively (Barnett 1995; Wiranidchapong 2006; Wiranidchapong 2008; Wiranidchapong 2009). The broad band characteristic indicates the hydrogen-bonded hydroxyl group with water entrapped in the crystal structure.

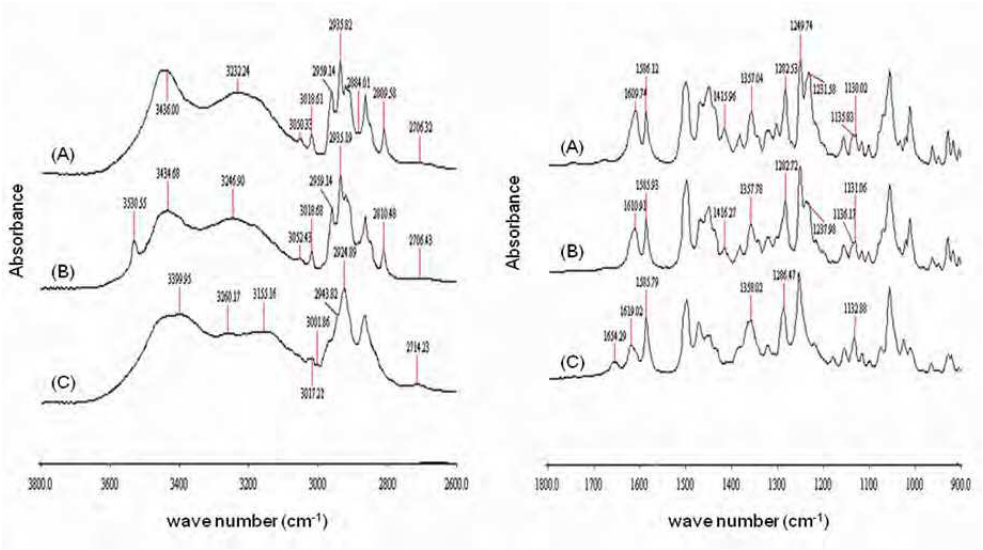

Fig. 8. FTIR spectra of E_2-hemihydrate (A); anhydrous E_2 (B); and the mixture of anhydrous E_2 with amorphous E_2 (C), recorded at room temperature in the range of 3800-2600 cm^{-1} (left) and 1800-900 cm^{-1} (right).

Anhydrous E_2 prepared by heating E_2-hemihydrate to 175 °C at 5 K/min displayed the peak around 3530 cm^{-1} in the FTIR spectrum. This peak corresponded to free hydroxyl group absorption (Kuo 2001a; Kuo 2001b; Wiranidchapong 2006; Wiranidchapong 2008; Wiranidchapong 2009). The appearance of this peak was agreed with the water loss during heating. However, broad bands centered at 3434.27 and 3245.29 cm^{-1} attributed to O-H stretching of hydroxyl group adjacent to C-17 and C-3 positions respectively in the E_2 chemical structure, were still observed.

For FTIR spectrum of E_2 heated to 220 °C at 5 K/min, which was presumably the mixture of anhydrous E_2 with amorphous E_2, the O-H stretching bands of hydroxyl groups adjacent to the C-17 and C-3 positions and C-H stretching vibration of aromatic ring in the regions of 3100-3000 cm^{-1} (Silverstein 1991) shifted to lower wavenumber when compared with those of E_2-hemihydrate and anhydrous E_2. Furthermore, three consecutive peaks in the range of 1655-1580 cm^{-1} attributed to absorption of the mixtures of tautomeric keto and enol forms (Silverstein 1991) were noticed in FTIR spectrum of E_2 heated to 220 °C whereas only two consecutive peaks in this region were observed in FTIR spectra of E_2-hemihydrate and anhydrous E_2. Due to the absorption peak in this region affected by physical state, electronic and mass effects of neighboring substitutes, conjugation, hydrogen bonding, and ring strain (Silverstein 1991), this might be the characteristics of amorphous E_2 blended with anhydrous

E_2. In addition, the peaks in the regions of 1300-900 cm^{-1} illustrated different shapes from those of E_2-hemihydrate, and anhydrous E_2.

According to drug dissolution and drug solubility in the polymer affecting the rate of drug released from either polymer membrane permeation- or polymer matrix diffusion-controlled release systems, solid state of E_2 dispersing in the polymer should also influence on the rate of E_2 release. Solid dispersion prepared by solvent evaporation is generally used to distribute drug into the polymeric matrix (Serajuddin 1999). Solid dispersions containing E_2 in ERS at 1 and 2 % w/w exhibited amorphous state of E_2 in the dispersion while those containing E_2 at 10, 20, and 30 % w/w illustrated crystalline state of E_2 in the dispersion (Wiranidchapong 2006). This interpretation was supported by photomicrographs of ERS, solid dispersion containing 1, 2, 10, 20, and 30 % w/w of E_2 in ERS and E_2 under polarized light microscope as shown in Figure 9. The absence of birefringence was observed in ERS and solid dispersions containing 1 and 2 % w/w of E_2. This is a characteristic of amorphous substance, which cannot turn plane polarized light and cannot reflect purple light to other wavelengths of visible lights. On the other hand, the birefringence was observed in solid dispersions containing 10, 20, and 30 % w/w of E_2 and E_2 crystal powder. This is a characteristic of crystalline substance, which is able to turn plane polarized light and reflect purple light to other visible wavelengths.

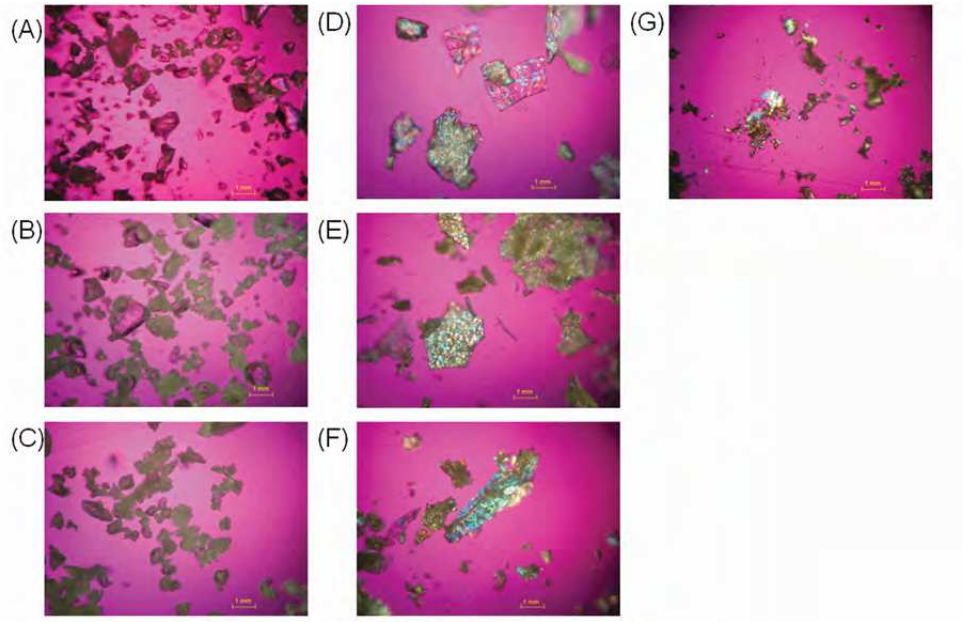

Fig. 9. Photomicrographs obtained from polarized light microscope: (A) ERS; solid dispersions containing E_2 in ERS at weight percent of (B) 1; (C) 2; (D) 10; (E) 20; (F) 30; and (G) E_2-hemihydrate (Reproduced from Wiranidchapong, 2006).

To compare with approximately 80 % of the E_2 released from the matrices containing E_2 at 10, 20, and 30 % w/w in the dispersion within 7 days, the matrices, which were composed of E_2 at 1 and 2 % w/w in the dispersions released approximately 60-80 % of the E_2 within 3

days (Wiranidchapong 2006). This study was in accordance with the finding of amorphous E_2 in the dispersion containing E_2 at 1 and 2 % w/w. Amorphous state is thermodynamically unstable. The molecular interactions of amorphous substance are weakened and usually gone into breaking. Therefore, amorphous E_2 exhibited higher dissolution rate than crystalline E_2, so that the rate of E_2 release from matrix containing amorphous E_2 is higher than that of the matrix containing crystalline E_2.

The polymorphic state of E_2 in the polymer matrix can be observed not only by polarized light microscope but also by DSC and/or MTDSC (modulated temperature differential scanning calorimetry) (Wiranidchapong 2006; Wiranidchapong 2008; Wiranidchapong 2009). To understand how DSC and/or MTDSC can differentiate between amorphous state and crystalline state of E_2 dispersing in the polymer matrix. Thermal behavior of solid dispersion containing E_2 in ERS should be explored.

5. Thermal behavior of E_2 in ERS solid dispersion

In general, T_g is one of thermal properties of an amorphous material observed by thermal analysis. Likewise, the melting point is a thermal property of a crystalline material. In the case of the amorphous E_2 existing in the polymer matrix, either E_2 or polymer in the matrix are amorphous materials. Thus, both amorphous E_2 and the polymer can manifest their T_g. A question is how the T_g behavior of this solid dispersion is. Which one between a single T_g or both T_g of amorphous E_2 and the polymer should be observed? For a solid dispersion composed of crystalline E_2 in the polymer matrix, what the temperature should be the melting point of E_2 in the dispersion? Does the polymer influence on the melting point of E_2? To understand the thermal behaviors of E_2 in ERS solid dispersion, the theory of the miscibility between the binary mixtures in which a polymer blend should be addressed.

5.1 T_g behavior described by the Gordon Taylor equation

In polymer sciences, the miscibility of a polymer blend composed of two amorphous polymers can be determined by thermal analysis. A single T_g point is an indication of full miscibility of a polymer blend (Kuo 2001a; Kuo 2001b; Maldonado-Santoyo 2004). On the contrary, an immiscible polymer blend exhibits more than one T_g representing T_g of amorphous pure polymers used as components (Kuo 2001a). In general, T_g of a miscible blend lies between T_g of the pure polymers, which can be predicted by Gordon-Taylor equation or its modified version equation (Maldonado-Santoyo 2004). Either T_g or weight fraction of binary polymer components are major factors in predicting the T_g of a miscible polymer blend by Gordon-Taylor equation and its modified version equation.

Gordon-Taylor equation has been proposed for the composition dependence on the T_g of miscible polymer blends derived under these assumptions (Schneider 1988);

1. The contacts due to the interaction between the components of the blend are responsible for conformational arrangement, free volume distribution, and conformational energy barriers.
2. The probabilities of binary contact are related to the volume fractions of the components, so that the composition dependence on the T_g has been related to the volume fractions (Ø) of the components.

The Gordon-Taylor equation with respect to the volume fraction ($Ø_2$) of the stiffer polymer component (with T_{g2}) has been defined as the following relationship (Schneider 1988);

$$\frac{T_g - T_{g1}}{T_{g2} - T_{g1}} = (1 + K_1)\emptyset_2 - (K_1 + K_2)\emptyset_2^2 + K_2\emptyset_2^3 \quad (15)$$

The parameters K_1 and K_2 are related to the difference of the T_g of the polymer components $(T_{g2} - T_{g1})$, so that

$$K_1 = \frac{K_1^*}{(T_{g2} - T_{g1})} \quad (16)$$

and

$$K_2 = \frac{K_2^*}{(T_{g2} - T_{g1})} \quad (17)$$

The system-specific constant K_1^* is related to the interaction energy differences between hetero- and homo-contacts, whereas K_2^* considers the energetic effects on the binary contacts of the molecular surrounding.

The ideal behavior of the polymer blend exhibits the equality of the different energetic effects. This means the identical energetic effects of both hetero- and homo-contacts and the equality of the contact energy of the molecular neighborhood. So both K_1^* and K_2^* are equal to zero in the idealized condition of the T_g behavior of miscible polymer blend. The Gordon-Taylor equation resulted from the idealized condition can be expressed;

$$\frac{T_g - T_{g1}}{T_{g2} - T_{g1}} = \emptyset_2 \quad (18)$$

$$T_g = \emptyset_2 T_{g2} + (1 - \emptyset_2) T_{g1} \quad (19)$$

Because of $\emptyset_1 + \emptyset_2 = 1$, and then

$$T_g = \emptyset_2 T_{g2} + \emptyset_1 T_{g1} \quad (20)$$

To express in term of the temperature-dependent weight fraction (w_i), the volume fractions ($\emptyset_i$) are given by the expression;

$$\emptyset_i = \frac{(\Delta\alpha_i \times w_i)/\rho_i}{\sum_i\{(\Delta\alpha_i \times w_i)/\rho_i\}} \quad (21)$$

where ρ_i is the density of the components and $\Delta\alpha_i$ is the difference between the expansion coefficients of the melt (L) and the glass (gl) at T_{gi} $(\Delta\alpha_i = \alpha_{L,i} - \alpha_{gl,i})$.

Introducing Equation (21) into Equation (20), yielding the Gordon-Taylor equation expressed in term of the temperature-dependent weight fraction as displayed;

$$T_g = \frac{\rho_2 \Delta\alpha_1 w_1 T_{g1} + \rho_1 \Delta\alpha_2 w_2 T_{g2}}{(\rho_2 \Delta\alpha_1 w_1 + \rho_1 \Delta\alpha_2 w_2)} \quad (22)$$

Due to $K = \frac{\rho_1 \Delta\alpha_2}{\rho_2 \Delta\alpha_1}$, so that Equation (22) can be rearranged as;

$$T_g = \frac{w_1 T_{g1} + K w_2 T_{g2}}{w_1 + K w_2} \quad (23)$$

In the case of polymer blends exhibiting the behavior deviating from the ideal behavior, the fit of Gordon-Taylor equation to experimental data fails. This suggests an interaction contribution to the Gordon-Taylor parameters (K). The Kwei equation is recommended in this case. The Kwei relation is identical to a second-order equation of the proposed model

expressed in Equation (15). It considers different energetic effects of the binary contact ($K_1 \neq 0$), but neglects the effects of the immediate neighborhood of contacts ($K_2 = 0$). Therefore, Equation (15) can be written under this assumption as shown;

$$\frac{T_g - T_{g1}}{T_{g2} - T_{g1}} = (1 + K_1)\emptyset_2 - K_1\emptyset_2^2 \tag{24}$$

Equation (24) can be illustrated in term of the corrected weight fraction (w_{ic}) as the following equations;

$$\frac{T_g - T_{g1}}{T_{g2} - T_{g1}} = (1 + K_1)w_{2c} - K_1 w_{2c}^2 \tag{25}$$

$$T_g = w_{1c}T_{g1} + w_{2c}T_{g2} + \left(T_{g2} - T_{g1}\right)(K_1 w_{2c} w_{1c}) \tag{26}$$

Due to $w_{1c} = w_1/(w_1 + Kw_2)$ and $w_{2c} = Kw_2/(w_1 + Kw_2)$, so that Equation (26) can be rewritten as displayed;

$$T_g = \frac{w_1 T_{g1} + Kw_2 T_{g2}}{w_1 + Kw_2} + \left(T_{g2} - T_{g1}\right)\frac{K_1 K w_2 w_1}{(w_1 + Kw_2)^2} \tag{27}$$

Because of $q = \left(T_{g2} - T_{g1}\right)\frac{K_1 K}{(w_1 + Kw_2)^2}$, then Equation (27) can be illustrated as;

$$T_g = \frac{w_1 T_{g1} + Kw_2 T_{g2}}{w_1 + Kw_2} + q w_2 w_1 \tag{28}$$

Equation (28) is the Kwei equation, which is the second order equation of the proposed model. The q parameter reflects the balance between breaking the intra bonding and forming the inter bonding. Normally the q parameter corresponds to the strength of hydrogen bonding. The q value of the polymer blend should depend on an entropy change corresponding to the change in the number of hydrogen bonding interactions. In the case of negative q value, it indicates that the self-associated hydrogen bonding is stronger than the inter-associated hydrogen bonding. In reciprocal way, the positive q value indicates that the self-associated hydrogen bonding is weaker than the inter-associated hydrogen bonding. The higher q value, the stronger hydrogen bonding (Kuo 2001a; Kuo 2001b).

The third order equation of the proposed model considers the contact interaction energies ($K_1 \neq 0$) and the influence of the molecular neighborhood on the contact energy ($K_2 \neq 0$), so that Equation (15) can be written in the term of the corrected weight fraction of the stiffer polymer (w_{2c}) as displayed below;

$$\frac{T_g - T_{g1}}{T_{g2} - T_{g1}} = (1 + K_1)w_{2c} - (K_1 + K_2)w_{2c}^2 + K_2 w_{2c}^3 \tag{29}$$

The Equation (29) can be resolved for the T_g of the blend as the following expression;

$$T_g = \frac{(1 - w_2)T_{g1} + Kw_2 T_{g2}}{1 + (K-1)w_2} + \frac{K_1^* K}{\{1 + (K-1)w_2\}^2} \times (1 - w_2)w_2 - \frac{-K_2^* K_2}{\{1 + (K-1)w_2\}^3} \times (1 - w_2)w_2^2 \tag{30}$$

Equation (30) is an extended Gordon-Taylor equation, which is written in term of the weight fraction of the stiffer polymer (w_2). Due to Equations (16) and (17), K_1^* and K_2^* are related to K_1 and K_2, respectively, so that the influence of the weight fraction of the components on the T_g is included both K_1 and K_2.

The application of Gordon-Taylor equation and its modified version equation has been extended to describe the T_g behavior of E_2 in ERS solid dispersion (Wiranidchapong 2006; Wiranidchapong 2008; Wiranidchapong 2009). The study revealed that solid dispersions containing E_2 in ERS at weight percent of 1-90 manifested a single T_g lying between the T_g of ERS (66.21 °C) and E_2 (83.77 °C) as displayed in Figure 10.

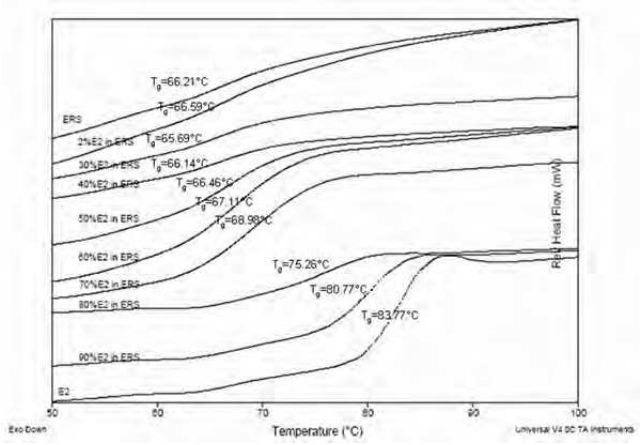

Fig. 10. T_g of E_2 in ERS solid dispersions at concentration range of 0-100 % w/w investigated by MTDSC with the program: heating to 182 °C, 10 K/min, cooling to 25 °C, 20 K/min, an isothermal period for 5 min at 25 °C, and finally heating to 250 °C, 5 K/min (Reproduced from Wiranidchapong, 2008).

In addition, the T_g shifted toward the T_g of E_2 when weight fractions of E_2 in the dispersions increased. This behavior was observed in E_2 in ERS solid dispersions investigated by MTDSC with the program of heating from 25 to 182 °C at 10 °C/min, cooling to 25 °C at 20 °C/min, an isothermal period for 5 min at 25 °C, and finally heating to 250°C at 5 °C/min. This heating program provided the transformation of E_2-hemihydrate into amorphous E_2 blended with ERS as the same as a blend of amorphous polymers. Thus, the T_g behavior of these blends could be described by the principle of Gordon-Taylor equation. However, the experimental T_g values were better fitted to Kwei equation than the Gordon-Taylor equation. The q value, the Kwei equation parameters, obtained from the curve-fitting was not equal to zero, which implied an interaction between E_2 and ERS in the blend.

5.2 The melting point behavior described by the flory-huggins theory

In the case of a crystalline polymer blended with an amorphous polymer, the melting point depression of a crystalline polymer in blend indicates the miscibility and interaction between the polymer components. Partially miscible or immiscible blends do not typically show the depression of melting point whereas a miscible blend displays the melting point depression when the content of amorphous polymer increases. The temperature reduction was a result of morphological effects and thermodynamic reasons (Kuo 2001a; Kuo 2001b). In a thermodynamically miscible blend, an amorphous polymer resides inside the interlamellar regions of a semi-crystalline polymer. It expands the interlamellar regions. The spherulite

radial growth rate, time to half volume crystallization and melting temperature of semi-crystalline component generally decrease as the concentration of the amorphous polymer increases. The mean field self-consistent theory used to a model of a blend containing di-block copolymers composing of crystallisable and amorphous copolymer blocks has been proposed. The free energy based on this theory can be expressed as a sum of free energy of free crystalline and amorphous blocks, entropy and enthalpy of interactions between these two blocks. For long chain polymers, the effect of the end groups can be ignored. The change in partial free energy of the crystals in a miscible blend (Δg_{2b}) can be expressed (Rostami 2000);

$$\Delta g_{2b} = \Delta g_2 + \Delta g_m \tag{31}$$

where Δg_2 is the change in partial free energy of crystalline unit of a homopolymer and Δg_m is the change in partial free energy of the mixture.

The equilibrium melting temperature is defined as the last temperature that infinitely long crystal melts. By definition, at the equilibrium melting temperature of the blends, where the last crystal melts, Δg_{2b} becomes zero, so that Equation (31) can be expressed as following equations;

$$\Delta g_2 = -\Delta g_m \tag{32}$$

$$\Delta h_2 - T_{mb}\Delta S_2 = -\Delta g_m \tag{33}$$

$$1 - \frac{T_{mb}\Delta S_2}{\Delta h_2} = \frac{-\Delta g_m}{\Delta h_2} \tag{34}$$

where Δh_2 is the heat of fusion of a crystalline polymer, T_{mb} is the equilibrium melting point of a blend, and ΔS_2 is the entropy of crystalline unit in a blend.

In condition of a narrow temperature range between T_{mb} and T_m, which is the equilibrium melting point of a crystalline polymer, it is reasonable to assume that Δh_2 and ΔS_2 are temperature independent hence;

$$T_m = \frac{\Delta h_2}{\Delta S_2} \tag{35}$$

Introducing Equation (35) into Equation (34), so that Equation (34) can be expressed as the following equation;

$$1 - \frac{T_{mb}}{T_m} = \frac{-\Delta g_m}{\Delta h_2} \tag{36}$$

A popular equation for Δg_m is given by the classic Flory-Huggins mean field model. When a crystalline polymer is designated as the second component in the mixture, the lattice model gives;

$$\Delta g_m = \frac{RT_{mb}V_2}{V_1}\left\{\ln\left(\frac{\phi_2}{r_2}\right) + \left(\frac{1}{r_2} - \frac{1}{r_1}\right)\phi_1\right\} + \frac{RT_{mb}V_2}{V_1}\lambda_{21}\phi_1^2 \tag{37}$$

where Ø is the volume fraction and r is the chain length of each component denoted by the subscript used. V_1 and V_2 are the molar volume of the amorphous unit and the crystalline unit, respectively. λ_{21} is the polymer-polymer interaction parameter. R is the universal gas constant. T_{mb} is the temperature of the blends. The term in the square bracket represents contribution from the combinatorial entropy to the chemical potential changes per mole of crystalline unit in the mixture. As a major contribution to the molar free energy changes of

the mixture is provided by the enthalpy term, which is the second term of Equation (37). The entropy contribution is neglected, so that Δg_m can be written in term of an approximate chemical potential form as displayed;

$$\Delta g_m = \frac{-RT_{mb}V_2}{V_1}\lambda_{21}\phi_1^2 \tag{38}$$

Substituting this approximated term into Equation (36) and rearranging, so that the resulting relationship is given as the following equation (Rostami 2000; Pimbert 2002);

$$\frac{1}{T_{mb}} - \frac{1}{T_m} = \frac{-RV_2\lambda_{21}\phi_1^2}{\Delta h_2 V_1} \tag{39}$$

According to $\lambda_{21} = \frac{BV_1}{RT_{mb}}$, Equation (39) can be written as the following expression (Nishi 1975; Kuo 2001a);

$$T_m - T_{mb} = \frac{-T_m BV_2\emptyset_1^2}{\Delta h_2} \tag{40}$$

where B is the interaction energy density characteristic of the polymer pair. The resulting equation, Equation (40), is the Nishi-Wang equation (Nishi 1975; Kuo 2001a; Kuo 2001b).
From the investigation of the E_2 melting point in solid dispersions containing E_2 in ERS at the concentration range of 0-100 % w/w (Wiranidchapong 2006; Wiranidchapong 2008), the melting point depression as a function of composition was revealed as displayed in Figure 11. The behavior of the E_2 melting point in ERS solid dispersion was in accordance with that of a crystalline polymer blended with an amorphous polymer. Fitting experimental melting point of E_2 in the dispersion to the Nishi-Wang equation exhibited good agreement between experimental values and predicted values, with randomly distributed residuals and the coefficient of determination (R^2) of 0.9804. In addition, B value obtained from curve-fitting was -0.281 J/(g*cm^3) (Wiranidchapong 2006; Wiranidchapong 2008). This indicated validity of the Nishi-Wang equation to predict the melting point of E_2 in ERS solid dispersions, miscibility and interaction between E_2 and ERS in the molten state.

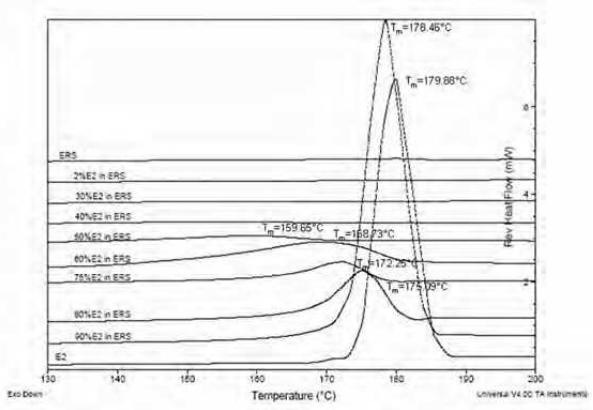

Fig. 11. The melting point depression of E_2 in ERS solid dispersions at concentration range of 0-100 % w/w investigated by MTDSC with the program of heating to 250 °C, 5 K/min (Reproduced from Wiranidchapong, 2006).

5.3 The interaction between E_2 and ERS in solid dispersion

Both Kwei equation and Nishi-Wang equation predicted an existence of a specific interaction between E_2 and ERS in the molten state. FTIR analysis was used to investigate the interaction between E_2 and ERS in solid dispersions. FTIR spectra of E_2 in ERS solid dispersions heated from 25-175 °C at 5 K/min were compared with those of anhydrous E_2 and ERS as illustrated in Figure 12. The peak around 3530 cm^{-1}, corresponding to free hydroxyl group absorption (Kuo 2001a; Kuo 2001b; Wiranidchapong 2006; Wiranidchapong 2008; Wiranidchapong 2009), in FTIR spectrum of anhydrous E_2 was also observed in that of 75 % w/w E_2 in ERS solid dispersion heated from 25-175 °C. This indicated the water loss during the heating process, so that the free hydroxyl group of E_2 was observed. Additionally, the band at 1732 cm^{-1} corresponding to the ester C=O stretching vibration of free carbonyl group (Pignatello 2002; Wiranidchapong 2006; Wiranidchapong 2008; Wiranidchapong 2009) was displayed in FTIR spectrum of ERS.

The interaction between E_2 and ERS was affirmed by the shift of broad band centered at 3434 cm^{-1}, attributed to O-H stretching of hydroxyl groups adjacent to C-17 positions in E_2, to 3411 cm^{-1} with a shoulder of the ester C=O stretching band in 75 %w/w E_2 in ERS solid dispersion heated from 25-175 °C. The shoulder around 1710 cm^{-1} corresponding to the hydrogen-bonded carbonyl group (Kuo 2001a; Kuo 2001b; Wiranidchapong 2006; Wiranidchapong 2008; Wiranidchapong 2009) suggested the inter-associated hydroxyl-carbonyl bond. The shoulder around 1710 cm^{-1} was also observed in FTIR spectra of 50 and 20 %w/w E_2 in ERS solid dispersions heated from 25-175 °C. Thus, the inter-associated hydrogen bonding between the free hydroxyl group of E_2 and the ester C=O group of ERS was occurred in solid dispersion of E_2 in ERS in the molten state in which water was removed from the E_2 crystal. This occurrence was in accordance with the prediction by Kwei equation and Nishi-Wang equation.

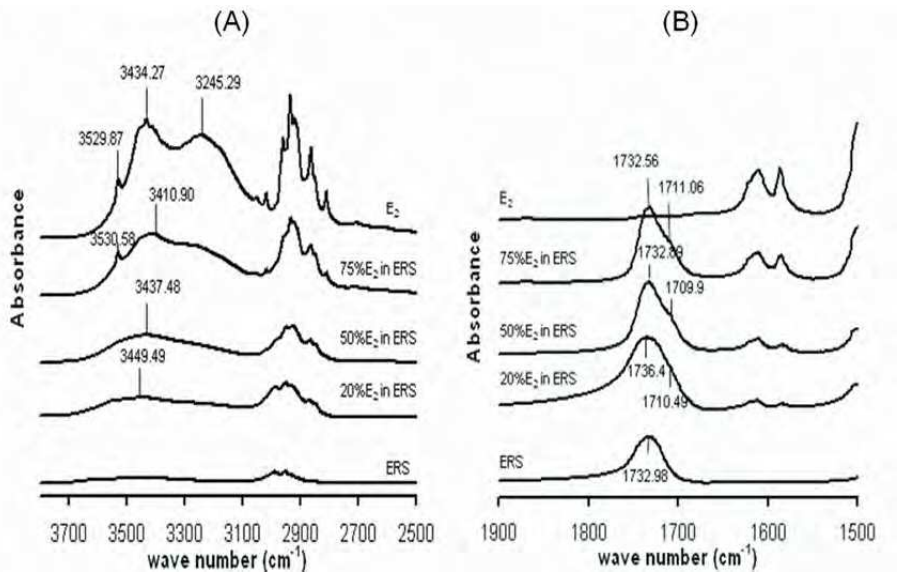

Fig. 12. FTIR spectra of E_2 in ERS solid dispersions at concentration range of 0-100 % w/w heated from 25-175 °C, 5 K/min, recorded at room temperature in the range of 3800-2600 cm^{-1} (A) and 1800-900 cm^{-1} (B) (Reproduced from Wiranidchapong, 2008).

6. Conclusions

E_2 is an essential steroid hormone that regulates numerous endocrine functions secreted during the reproductive years. Early phase in menopause symptoms can be relieved by administration of E_2 mimic the menstrual cycle. The treatment goal requires the lowest effective dose delivered into the blood circulation at a constant rate. This manner can prevent estrogen-insufficient symptoms and/or estrogen-excess symptoms according to peak and trough pattern of plasma estrogen concentration versus time profile. Polymer matrix diffusion controlled-release drug delivery system can provide a relatively constant rate of E_2 release. The accomplishment of a constant release is a result of the inherent solubility of E_2 providing the drug dissolution controlled-release system.
Polymorphic state of E_2 dispersing in the polymer matrix directly affects the solubility of E_2 in the surrounding medium and consequently the rate of E_2 released. Thermal analysis can be used to verify the polymorphic state of E_2 dispersing in the polymer matrix. In the case of amorphous E_2 dispersing in the polymer matrix, the T_g behavior can be described by the principle of Gordon-Taylor equation. On the other hand, the melting point depression of crystalline E_2 dispersing in the polymer matrix can be described by the Flory-Huggins theory. Additionally the interaction between E_2 and ERS used as a polymer matrix can be predicted by both theories.

7. Acknowledgment

This work is performed to celebrate Associate Professor Poj Kulvanich's sixty birthday. I wish to express my gratitude to my Ph.D. supervisor, Associate Professor Poj Kulvanich for providing me an opportunity to do the research at School of Pharmacy, University of Otago, New Zealand in 2005. The virtue of this work is given to Professor Ian Tucker, who makes me know how valuable the fitting model is. My acknowledgment is extended to Professor Thomas Rades, who firstly introduces me the principle of Gordon-Taylor equation. My special thanks are given to Boonta Chutvirasakul, lecturer in Pharmaceutical Chemistry, Faculty of Pharmacy, Srinakharinwirot University for her assistance to proof the language of this work. Finally, I would like to express my gratitude to my mother and older brother for their support and encouragement.

8. References

Abdul, S., and Poddar, S. S. (2004). "A flexible technology for modified release of drugs: Multi layered tablets." J Control Release 97: 393-405.

Anderson, P. O., Knoben, J. E., and Troutman, W. G. (2002). Handbook of clinical drug data, McGraw-Hill.

Andersson, T. L. G., Stehle, B., Davidsson, B., and Höglund, P. (2000). "Drug concentration effect relationship of estradiol from two matrix transdermal delivery systems: Menorest® and Climara®." Maturitas 35: 245-252.

Barnett, S. M., Butler, I. S., Top, S., and Jaouen, G. (1995). "Pressure-tuning infrared and solution Raman spectroscopic studies of 17β-estradiol and several A-ring and 17α-ethynylestradiol derivatives." Vib Spectros 8: 263-277.

Bawaarshi-Hassar, R. N., Hussain, A. A., and Crooks, P. A. (1989). "Nasal absorption and metabolism of progesterone and 17beta-estradiol in the rat." Drug Matab Dispos 17: 248.

Boyd, R. A., Zegarac, E. A., Eldon, M. A. (2003). "The effect of food on the bioavailability of norethindrone and ethinyl estradiol from norethindrone acetate/ethinyl estradiol tablets intended for continuous hormone replacement therapy." J Clin Pharmacol 43(1): 52-58.

Chandrasekaran, S. K., and Paul, D. R. (1982). "Dissolution-controlled transport from dispersed matrixes." J Pharm Sci 71: 1399-1402.

Chien, Y. W. (1982). Novel drug delivery systems: Fundamentals, developmental concepts and biomedical assessments. New York, Marcel Dekker.

Chien, Y. W. (1989). "Rate-control drug delivery systems: Controlled release vs. sustained release." Medical Progress Through Technology 15: 21-46.

Chien, Y. W. (1992). Novel drug delivery system. New York, Marcel Dekker.

Cobby, J., Mayershon, M., and Walker, G. C. (1974). "Influence of shape factors on kinetics of drug release from matrix tablets: I. Theoretical." J Pharm Sci 63: 725-733.

Conte, U., and Maggi, L. (1996). "Modulation of the dissolution profiles from Geomatrix© multi-layer matrix tablets containing drugs of different solubility." Biomaterials 17: 889-896.

Conte, U., and Maggi, L. (2000). "A flexible technology for the linear, pulsatile and delayed release of drugs, allowing for easy accommodation of difficult in vitro targets." J Control Release 64: 263-268.

Conte, U., Maggi, L., Colombo, P., and La Manna, A. (1993). "Multi-layered hydrophilic matrices as constant release devices (Geomatrix™ system)." J Control Release 26: 39-47.

Costa, P., and Lobo, J. M. S. (2001). "Modeling and comparison of dissolution profiles." Eur J Pharm Sci 13: 123-133.

Croxatto, H. B., et. al. (1981). "Plasma levels of levonorgestrel in women during long-term use of Norplant." Contraception 23(197).

Danckwerts, M., and Fassihi, A. (1991). "Implantable controlled release drug delivery systems: A review." Drug Dev Ind Pharm 17: 1465-1502.

Dash, A. K., and Cudworth II, G. C. (1998). "Therapeutic applications of implantable drug delivery systems." Journal of Pharmacological and Toxicological Methods 40(1): 1-12.

Diaz, S., et. al. (1982). "A five-year clinical trial of levonorgestrel silastic implants (Norplant)." Contraception 25: 447.

Dunn, J. F. (1983). Transport of estrogens in human plasma. Catechol Estrogens. G. R. Merriam. New York, Raven: 167-176.

Grant, J., and Park, G. S. (1968). Diffusion in polymers. New York, Academic Press.

Hsieh, D. S. T., Rhine, W. D., and Langer, R. (1983). "Zero-order controlled-release polymer matrices for micro- and macro-molecules." J Pharm Sci 72: 17-22.

Hsieh, D. S. T., Smith, N., and Chien, Y. W. (1987). "Subcutaneous controlled delivery of estradiol by Compudose implants: In vitro and in vivo evaluations." Drug Dev Ind Pharm 13: 2651-2666.

Iwamori, M. (2005). "Estrogen sulfatase." Methods Enzymol 400: 293-302.

Kim, C.-J. (2000). Drug dissolution/diffusion controlled systems. Controlled release dosage form design. C.-J. Kim. Pennsylvania, Technomic Publishing: 75-82.

Kuhl, H. (2005). "Pharmacology of estrogens and progestogens: Influence of different routes of administration." Climacteric 8(Suppl 1): 3-63.

Kuhnz, W., Gansau, C., and Mahler, M. (1993). "Pharmacokinetics of estradiol, free and total estrone, in young women following single intraveneous and oral administration of 17β-estradiol." Arzneim-Forsch/Drug Res 43: 966-973.

Kuo, S. W., and Chang, F. C. (2001a). "Miscibility and hydrogen bonding in blends of poly (vinylphenol-co-methyl methacrylate) with poly (ethylene oxide)." Macomolecules 34: 4089-4097.

Kuo, S. W., Huang, C. F., and Chang, F. C. (2001b). "Study of hydrogen-bonding strength in poly (ε-caprolactone) blends by DSC and FTIR." J Polym Sci Part B: Polym Phys 39: 1348-1359.

Latsch, S., Selzer, T., Fink, L., and Kreuter, J. (2003). "Crystallization of estradiol containing TDDS determined by isothermal microcalorimetry, x-ray diffraction, and optical microscopy." Eur J Pharm Biopharm 56: 43-52.

Longcope, C., Gorbach, S., Goldin, B., Woods, M., Dwyer, J., and Warram, J. (1985). "The metabolism of estradiol; oral compared to intraveneous administration." J Steroid Biochem 23: 1065-1070.

Maggi, L., Bruni, R., and Conte, U. (2000). "High molecular weight polyethylene oxides (PEOs) as an alternative to HPMC in controlled release dosage forms." Int J Pharm 195: 229-238.

Maldonado-Santoyo, M., et al. (2004). "Miscibility behavior and hydrogen bonding in blends of poly (vinyl phenyl ketone hydrogenated) and poly (2-ethyl-2-oxazoline)." J Polym Sci Part B: Polym Phys 42: 636-645.

Margolis, M. B. (2010). "How drug delivery and pharmacokinetics impact estrogen therapy." The Female Patient(Suppl 5): 1-8.

Meli, A., Cargill, D. I., Giannina, T., and Steinetz, B. G. (1968). "Studies on the transport of estrogens by the rat small intestine in vivo." Proc Soc Exp Biol Med 129: 937-944.

Mueck, A. O., and Seeger, H. (2003). "Smoking, estradiol metabolism and hormone replacement therapy." Arzneimittelforschung 53(1): 1-11.

Munoz, A. (1999). "Oesclim©: An advanced delivery system for HRT." Maturitas 33(s39-s47).

Niazi, S. K. (2007). Handbook of Preformulation: Chemical, Biological, and Botanical Drugs. New York, Informa Healthcare USA.

Nishi, T., and Wang, T. T. (1975). "Melting point depression and kinetic effects of cooling on crystallization in poly(vinylidine fluoride)-poly(methyl methacrylate) mixtures." Macromolecules 8: 909-915.

Paoletti, A. M., Pilia, I., Nannipieri, F., Bigini, C., and Melis, G. B. (2001). "Comparison of pharmacokinetic profiles of a 17β-estradiol gel 0.6 mg/g (Gelestra) with a transdermal delivery system (Estraderm TTS 50) in postmenopausal women at steady state." Maturitas 40: 203-209.

Pardridge, W. M. (1986). "Serum bioavailability of sex steroid hormones." Clin Endocrinol Metab 15: 259-278.

Park, J.-S., Kang, H. W., Park, S. J., and Kim, C-K. (2005). "Use of CP/MAS solid-state NMR for the characterization of solvate molecules within estradiol crystal forms." Eur J Pharm Biopharm 60: 407-412.

Pentikis, H. S., Mullin, M. E., Howard, M., Boutouyrie, B., and Rhodes, G. (1998). "Evaluation of the bioavailability and dose proportionality of three formulations of a combination estrogen and progestin adhesive-based matrix transdermal delivery system." Curr Ther Res 59: 681-691.

Pignatello, F., M., and Puglisi, G. (2002). "Preparation of solid dispersions of nonsteroidal anti-inflammatory drugs with acrylic polymers and studies on mechanisms of drug-polymer interactions." AAPS Pharm Sci Tech 3: 1-11.

Pimbert, S., Avignon-Poquillon, L., and Levesque, G. (2002). "Calorimetric study of fluorinated methacrylic and vinyl polymer blends: Part 2: Correlation between

miscibility, chemical structure and c_{12} interaction parameter in binary systems." Polymer 43: 3295-3302.

Plowchalk, D. R., and Teeguarden, J. (2002). "Development of a physiologically based pharmacokinetic model for estradiol in rats and humans: A biologically motivated quantitative framework for evaluating responses to estradiol and other endocrine-active compounds." Toxicological Sciences 69: 60-78.

Rippie, E. G., and Johnson, J. R. (1969). "Regulation of dissolution rate by pellet geometry." J Pharm Sci 58: 428-431.

Rohr, U. D., Nauert. C., and Stehle, B. (1999). "17β-estradiol delivered by three different matrix patches 50 mg/day: A three way cross-over study in 21 postmenopausal women." Maturitas 33: 45-48.

Rostami, S. D. (2000). "Advances in theory of equilibrium melting point depression in miscible polymer blends." Eur Polym J 36: 2285-2290.

Schneider, H. A. (1988). "The Gordon-Taylor equation. Additivity and interaction in compatible polymer blends." Makromol Chem 189: 1941-1955.

Segal, S. J. (1983). "The development of Norplant implants." Studies in Family Planning 14: 161.

Serajuddin, A. T. M. (1999). "Solid dispersion of poorly water-soluble drugs: Early promises, subsequent problems, and recent breakthroughs." J Pharm Sci 88: 1058-1066.

Shargel, L., and Yu, A. (1999). Applied biopharmaceutics and pharmacokinetics. New Jersey, Prentice-Hall International.

Siepmann, J., and Peppas, N. (2001). "Modeling of drug release from delivery systems based on hydroxypropyl methylcellulose (HPMC)." Adv Drug Deliv Rev 48: 139-157.

Silverstein, R. M., Bessler, G. C., and Morrill, T. C. (1991). Infrared spectrometry. Spectrometric identification of organic compounds. J. Stiefel. Singapore, John Wiley and Sons: 91-164.

Utian, W. H., Archer, D. F., Bachmann, G. A., et al; North American Menopause Society (2008). "Estrogen and progestogen use in postmenopausal women: July 2008 position statement of the North American Menopause Society." Menopause 15(4(pt 1)): 584-602.

Vandelli, M. A., and Cameroni, R. (1993a). "Selective coating of cylindrical matrices with a central hole. I. An interpretation of the swelling process." Int J Pharm 100: 107-114.

Vandelli, M. A., Coppi, G., and Cameroni, R. (1993b). "Selective coating of cylindrical matrices with a central hole. II. An interpretation of the release process." Int J Pharm 100: 115-121.

Variankaval, N. E., Jacob, K. I., and Dinh, S. M. (2000). "Characterization of crystal forms of β-estradiol-thermal analysis, Raman microscopy, X-ray analysis and solid-state NMR." J Cryst Growth 217: 320-331.

Weiner, E., et. al. (1981). "Plasma levels of d-norgestrel after oral administration." Contraception 23: 197.

Wiranidchapong, C. (2006). Development of 17b-estradiol and norethindrone implants using acrylate polymers as release controlling agent Pharmaceutics. Bangkok, Chulalongkorn University. Doctor of Philosophy in Pharmaceutics: 107.

Wiranidchapong, C., Rades, T., Tucker, I. G., Kulvanich, P. (2009). "Method of preparation does not affect the miscibility between steroid hormone and polymethacrylate." Thermochimica Acta 485: 57-64.

Wiranidchapong, C., Tucker, I. G., Rades, T., Kulvanich, P. (2008). "Miscibility and interactions between 17b-estradiol and Eudragit® RS in solid dispersion." J Pharm Sci 97(11): 4879-4888.

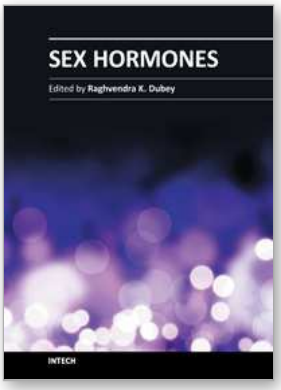

Sex Hormones

Edited by Prof. Raghvendra Dubey

ISBN 978-953-307-856-4
Hard cover, 430 pages
Publisher InTech
Published online 08, February, 2012
Published in print edition February, 2012

Sex Hormones not only regulate reproductive function, but they also play a prominent role in the biology and physiology of several organs/tissues and in the pathophysiology of several diseases. During the last two decades, the information on the mechanisms of action of sex hormones, such as estrogens and androgens, has rapidly evolved from the conventional nuclear receptor dependent mechanisms to include additional non-nuclear, non-genomic and receptor-independent mechanisms. This highlights the need to update the current knowledge on sex hormones and their mode of action. Increasing evidence that exogenous/epigenetic factors can influence sex hormone production and action highlights the need to update our knowledge on the mechanisms involved. This book provides a systematic and updated overview of the male/female sex-hormones and their impact in the biology and physiology of various organs. Additionally, the book discusses their positive and negative association with the pathophysiology of various diseases (e.g. osteoporosis, cardiovascular-disease, hypogonadism, reproduction, cancer) and their therapeutic potential.

INTECH
open science | open minds

InTech Europe
University Campus STeP Ri
Slavka Krautzeka 83/A
51000 Rijeka, Croatia
Phone: +385 (51) 770 447
Fax: +385 (51) 686 166
www.intechopen.com

InTech China
Unit 405, Office Block, Hotel Equatorial Shanghai
No.65, Yan An Road (West), Shanghai, 200040, China
中国上海市延安西路65号上海国际贵都大饭店办公楼405单元
Phone: +86-21-62489820
Fax: +86-21-62489821